DOI: 10.1002/ejic.201000527

Heteroepitaxial Growth of ZnO Nanorod Arrays on GaAs (111) Substrates by Electrochemical Deposition

Hai Bo Zeng,*[a] Yoshio Bando,[a] Xi Jin Xu,*[a] Liang Li,[a] Tian You Zhai,[a] Xiao Sheng Fang,[a] and Dmitri Golberg[a]

Keywords: Zinc / Nanostructures / Electrochemical deposition / Epitaxial growth / Crystal growth

Heteroepitaxial growth of well-aligned ZnO nanorod arrays on GaAs (111) substrates was achieved through electrochemical deposition at low temperature without any buffer layers for the first time. Structural analysis demonstrated the epitaxial orientation relationship of ZnO(0001)//GaAs(111). The rod density was dependent on the applied current density. These ZnO nanorods had high crystalline quality and exhibited strong UV near-edge photoluminescence with a 106 meV full-width at half-maximum and very weak deep level emission. Furthermore, the patterned growth was facially implemented by using surface masks on cathode substrates. These results are envisaged to advance the development of ZnO nanorod-based heterojunctions and their applications in optoelectronics.

Introduction

Zinc oxide (ZnO) nanomaterials have attracted wide attention due to their potential applications in many fields, such as ultraviolet (UV) laser and light-emitting devices, electron field emitters, photocatalysts, and energy generators.[1–6] Among them, one of the most important prospects is the application of ZnO nanomaterials as UV and blue optoelectronic nanodevices, since their exciton binding energy is about 60 meV, which is larger than that of other widely used semiconductors, e. g. GaN (26 meV) or ZnSe (20 meV), and it also exceeds the room-temperature thermal energy (25 meV). Recently, both ZnO epitaxial films and nanowires have shown excellent optical characteristics.[7,8] Furthermore, alloying of ZnO with Mg and Cd has been implemented to tune the band gap energy.[9,10] These two aspects favor its application in optoelectronics. However, the difficulty of p-type doping in ZnO has greatly impeded the fabrication of ZnO p-n homojunctions and thus blocked the further development of related optoelectronic devices, such as light-emitting diodes (LEDs).[11]

Recently, as an alternative approach, heterojunctions combining ZnO nanowires with other well developed p-type semiconductors have attracted great attention. Typically, the Yi[12] and Myoung[13] groups epitaxially grew vertical ZnO nanowire arrays on Mg doped p-type GaN films, forming a heterojunction LED with blue electroluminescence emission.[12] In line with these ideas, p-type Si was also utilized, including vertically growing[14,15] or placing in parallel[16] ZnO nanowires on p-type Si substrates to form p-n junctions and LEDs. However, as a representative second-generation semiconductor material, GaAs has seldom been reported to merge with ZnO nanowires, although ZnO thin films have been grown on GaAs substrates.[17–19]

Here, for the first time, we report the electrochemical deposition (ECD) growth of vertical ZnO nanorods on GaAs (111) substrates at a low temperature and without any buffer layer. The nanorods are of high crystalline and optical quality. Furthermore, the patterned growth was facially demonstrated by using surface masks. These results would advance the development of ZnO nanorod-based heterojunctions and their applications in optoelectronics.

Results and Discussion

Figure 1a presents the low-magnification SEM image of ZnO nanorods grown on GaAs substrates. These rods have diameters and lengths of approximately 250 nm and 2.5 μm, respectively. The rod distribution is very homogeneous on the whole substrate. Most rods are vertically aligned on the GaAs substrate, which is further revealed by the high magnification SEM image in Figure 1b. As a typical character, the rod density is relatively low relative to that obtained by syntheses on other epitaxial substrates, such as GaN and Si,[20,21] where the ZnO nanowires usually cover the whole substrate surface. However, the verticality achieved here is really perfect. Furthermore, the rod density can be tuned by the applied current density, as shown in Figure 2. Typically, the densities corresponding to current densities of 1.0, 0.8, and 0.6 mA/cm^2 are about 185, 70, and 25 rods per

[a] International Center for Materials Nanoarchitectonics (MANA), National Institute for Materials Science (NIMS), Namiki 1-1, Tsukuba, Ibaraki 305-0044, Japan
E-mail: ZENG.Haibo@nims.go.jp
XU.Xijin@nims.go.jp

Supporting information for this article is available on the WWW under http://dx.doi.org/10.1002/ejic.201000527.

100 μm^2, respectively. The rod density decreases with the applied current density as shown in Figure 2g, but the change in rod diameter is negligible.

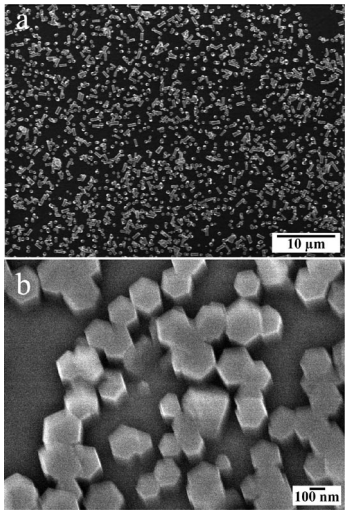

Figure 1. Typical views of ZnO nanorods electrodeposited on a GaAs (111) substrate: (a) Low-magnification SEM image, showing the large-scale production and homogeneous distribution of nanorods. (b) High-magnification SEM image with a 30 °C tilting angle, revealing the nanorod morphology and the perfect verticality of the rods to the substrate.

The notable hexagonal faceting and verticality of nanorods indicate that they are of high crystalline quality and are oriented along the *c* axis, as further confirmed by TEM analyses shown in Figure 3. Figure 3a shows the perfect top view of a hexagonal facet of a standing nanorod. The corresponding EDS spectrum in Figure 3b confirms the pure ZnO composition; no impurities are detected. This demonstrates that there is no element diffusion from the substrate into the nanorods during the growth. The latter usually takes place in high-temperature chemical vapor deposition (CVD) growth of ZnO nanowires on GaN and Si substrates, and thus greatly affects their optical/electronic properties.[19] Figure 3c presents the low-magnification side-view TEM image of a ZnO nanorod. The nanorod has a smooth surface and is slightly taperied along the axial direction. The HRTEM image in Figure 3d demonstrates the monocrystalline character and axial direction along the [0001] orientation; no obvious defects are observed in the whole body of the rod.

As a matter of fact, ZnO can be synthesized electrochemically from aqueous solutions of zinc salts. In 1996, Izaki et al.[22] and Peulon et al.[23] independently discovered methods to electrodeposit crystalline ZnO thin films, employing cathodic reduction of the nitrate ion and dissolved oxygen, respectively. ZnO can be grown cathodically under a range of deposition conditions from –0.76 to 0.88 V vs. the normal hydrogen electrode (NHE) at pH = 0.[24] The electrochemical formation of ZnO nanorods has been explained by Equations (1) and (2).[4,20] The reduction of nitrate ions from NO^{3-} to NO^{2-} and appearance of more hydroxy ions (OH^-) in the electrolyte would lead to the formation of

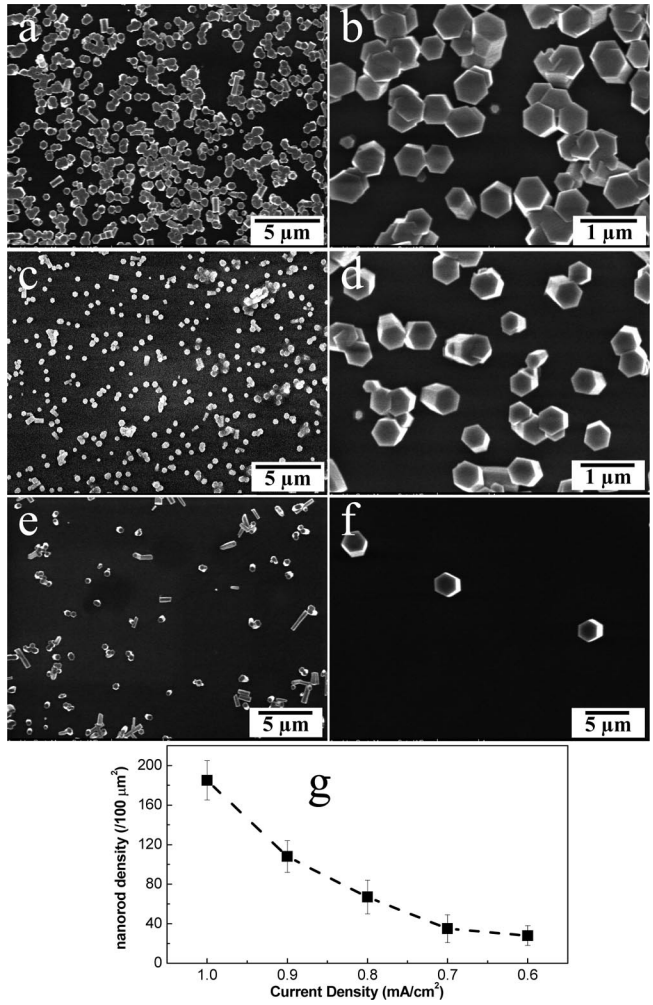

Figure 2. Current density dependence of rod density. Low- and high-magnification SEM images of ZnO nanorods prepared by electrodeposition with different deposition current densities: (a) and (b), 1.0 mA/cm^2; (c) and (d), 0.8 mA/cm^2; (e) and (f), 0.6 mA/cm^2. (g) Nanorod density vs. deposition current density.

$Zn(OH)_2$ and then of ZnO on the cathode by a simultaneous dehydration process. The preferential growth of nanorods along the *c* axis is favored by the polarized character of ZnO. The positively Zn^{2+}-terminated and negatively O^{2-}-terminated polar surfaces induce a net dipole moment along the *c* axis. Thus, the surface energy of the polar (0001) plane is higher than those of nonpolar planes, leading to growth along the *c* axis.

$$NO_3^- + H_2O + e^- \rightarrow NO_2^- + 2OH^- \quad (1)$$

$$Zn^{2+} + 2HO^- \rightarrow ZnO + H_2O \quad (2)$$

From the high-magnification SEM images of ZnO nanorods in Figures 1b and 2b–f, it can be observed that the undeposited parts are very clean, and no nanoparticles or buffer-layer-like thin films are formed on the substrate during ECD processes. Previously, we observed that many ZnO nanoparticles were formed on ITO substrates in the initial stage of the ECD process, and then acted as a buffer layer for subsequent growth of well-aligned ZnO nanowire ar-

rays.[4] Here, the ZnO nanorods were abruptly grown on the GaAs (111) substrates, which demonstrates heteroepitaxial growth. Combining with the clear faceting and [0001] growth orientation of ZnO nanorods in agreement with the SEM and TEM observations discussed above, we conclude that ZnO nanorods were epitaxially grown on the GaAs(111) substrate with the following orientation relationship:

ZnO(0001)//GaAs(111),
ZnO[11–20]//GaAs[01–1],
ZnO[10–10]//GaAs[11–2].

The epitaxial interface and matching configuration are presented in Figure 4. It is known that wurtzite ZnO has a hexagonal structure with the lattice parameters a = 0.32496 nm, c = 0.52065 nm, while zinc blende GaAs has a cubic structure with a = 0.56532 nm. The lattice mismatch in such configuration is –18.7%. The negative sign means that the atom spacing on the ZnO (0001) plane is smaller than that on the GaAs (111) plane. The c axis of the ZnO layer is parallel to the [111] axis of the GaAs substrate. The lattice strain in heteroepitaxial layers will appear due to the mismatch of lattice constants between the grown layer and the substrate material.[25] As revealed by the SEM image, the ZnO nanorods grown by ECD on a GaAs substrate are relatively sparse, although 1.0 mA/cm^2 is a suitable current density for the well-defined ZnO ECD growth. In contrast, ZnO nanowire arrays electrodeposited on a Si substrate with the ZnO nanocrystal buffer layer can be very dense under the same conditions, as shown in Figure S1. Here, an unavoidably low nucleation rate could be induced by the large lattice mismatches, which leads to a high nucleation energy for epitaxial growth from the electrolytes. In fact, many ZnO nanorods were found to form in the solution after the ECD process. The decreasing current density further depresses the nucleation rate, resulting in a lower nanorod density on the substrates, as shown in Figure 2.

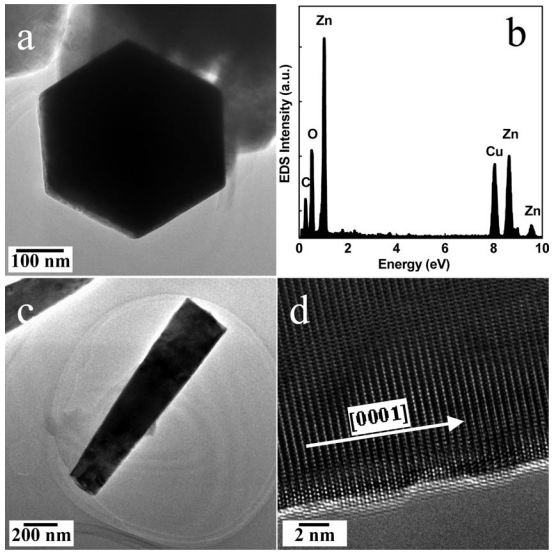

Figure 3. TEM characterizations of ZnO nanorods: (a) and (b) Top-view TEM image and EDS spectrum of a vertically standing rod, exhibiting perfect hexagonal faceting and pure ZnO composition. (c) and (d) Side-view TEM and HRTEM images of a lying rod, revealing single-crystalline features.

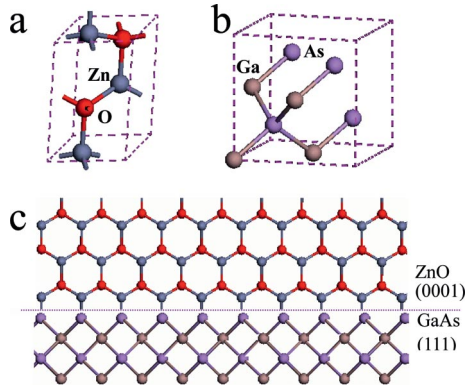

Figure 4. Unit cell structures of hexagonal ZnO (a) and cubic GaAs (b), and a sketch mapping the epitaxial orientation relationship between ZnO and a GaAs substrate (c).

Photoluminescence (PL) measurements were carried out at room temperature with a 325 nm He-Cd laser as the excitation source. The PL spectrum of nanorods grown under a current density of 1.0 mA/cm^2 (corresponding to Figure 2a and b) is shown in Figure 5. Ultraviolet (UV) emission with a peak energy of 3.23 eV and a full-width at half-maximum (FWHM) of 106 meV is dominantly observed. This FWHM is slightly smaller than other reported values, indicating the high quality of the near-band-edge (NBE) emission, typically 120 meV for a ZnO thin film grown on GaAs by molecular-beam epitaxy (MBE).[26] The visible emission related to the deep level (DL) defects is very weak.[2,27,28] The ratio of the peak intensities of NBE to that of DL, that is NBE/DL, is as high as 20 even at room temperature, which is slightly lower than those for high-quality thin films prepared by MBE (about 60), but higher than those for the films made by metalorganic chemical vapor deposition (MOCVD) (about 5).[9] These structural and PL results demonstrate that the ZnO nanorods grown by ECD on a GaAs substrate have well-defined crystalline and optical qualities, thus they have decent potentials in UV lighting or LED applications, especially when considering the high level of development of n-type doping of ZnO and p-type doping of GaAs.

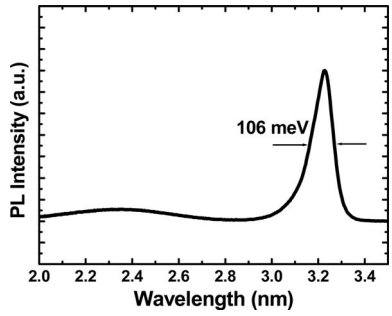

Figure 5. Room-temperature photoluminescence spectrum of ZnO nanorods grown by ECD on a GaAs substrate under an 1.0 mA/cm^2 current density.

Furthermore, patterned growth has usually been explored for practical applications. In fact, it can be easily achieved on such ECD-grown ZnO nanorods by utilizing preformed photoresist masks on substrates. The results are presented in Figure 6. ECD growth on GaAs substrates with holes and line grooves results in ZnO nanorod arrays (Figures 6a and b) and nanorod lines (Figures 6c and d), respectively. The size of holes and grooves has an obvious effect on the resulting nanorods. For the larger vacancy mask, nanorod bundles form preferably, as shown in Figures 6a and c. With decreasing mask size, the nanorods in Figure 6b become well separated and aligned on substrates and the nanorod line in Figure 6d becomes thinner (a width of nearly one rod). The inset in Figure 6b shows the perfect hexagonal faceting, indicating the high quality of the nanorods. Such facial patterning growth would benefit the fabrication of ZnO nanorod GaAs heterojunction devices and hence related optoelectronic applications.

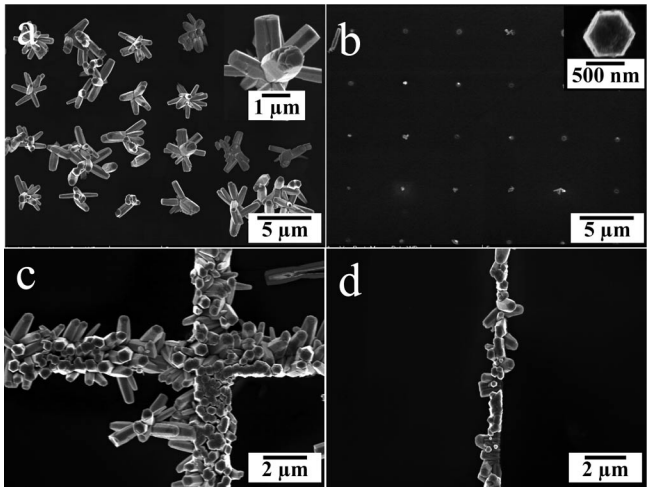

Figure 6. SEM images of patterned ZnO nanorods on GaAs substrates with photoresist masks of different configurations: holes with diameters of 1 μm (a) and 500 nm (b); grooves with line widths of 2 μm (c) and 500 nm (d). The inset shows a single rod standing on the substrate under larger magnification.

Conclusions

We report on the electrochemical deposition of vertical ZnO nanorods on GaAs (111) substrates at low temperature without any buffer layer for the first time. The structural analysis demonstrated the epitaxial orientations of ZnO(0001)//GaAs(111), ZnO[11–20]//GaAs[01–1], and ZnO[10–10]//GaAs[11–2]. The ZnO nanorods have high crystalline quality and exhibit strong UV near-edge emission with 106 meV full-width at half-maximum. Furthermore, patterned growth can be facially achieved by using surface masks. These results would promote the development of heterojunctions based on ZnO nanorods and their applications in optoelectronics.

Experimental Section

Galvanostatic cathodic deposition was employed on the substrates (cathode) at a current range of 0.8–1.5 mA. Zinc sheets (99.99% purity) acted as the anode, and the electrolyte solution was aqueous zinc nitrate (0.05 M). A Si-doped n-type GaAs (111) substrate was used as the cathode. The pH value of the solution was about 6. The deposition temperature was fixed at 70 °C by means of a water bath, and the deposition time was 1 h. For the patterned growth of nanorods, patterned substrates were used as cathodes for ECD growth. The conventional photoresist was firstly spin coated onto the substrates and then transformed into hole or line groove patterns by a normal photolithography process. The samples were characterized by field emission scanning electron microscopy (FE-SEM, FEI Sirion 200), X-ray diffraction (XRD, Philips X′Pert, Cu KR line: 0.15419 nm), and transmission electron microscopy (HRTEM, JEOL JEM-3000F). Optical properties were studied by PL spectra excited by the 325 nm line of a He-Cd laser.

Supporting Information (see footnote on the first page of this article): SEM image of ZnO nanowire arrays electrodeposited on a Si substrate with the ZnO nanocrystal buffer layer under a current density of 1.0 mA/cm^2.

Acknowledgments

This work was supported by the Japan Society for the Promotion of Science (JSPS) in the form of a fellowship tenable at the National Institute for Materials Science (NIMS), Tsukuba, Japan (H. B. Zeng and T. Y. Zhai). It was also in part supported by the World Premier International Center for Materials Nanoarchitectonics (MANA) of the National Institute for Materials Science (NIMS), Tsukuba, Japan.

[1] M. H. Huang, S. Mao, H. Feick, H. Q. Yan, Y. Y. Wu, H. Kind, E. Weber, R. Russo, P. D. Yang, *Science* **2001**, *292*, 1897.
[2] R. S. Yang, Y. Qin, L. M. Dai, Z. L. Wang, *Nat. Nanotechnol.* **2008**, *4*, *34*.
[3] Y. Qin, X. Wang, Z. L. Wang, *Nature* **2008**, *451*, 809.
[4] H. B. Zeng, X. J. Xu, Y. Bando, U. K. Gautam, T. Y. Zhai, X. S. Fang, B. D. Liu, D. Golberg, *Adv. Funct. Mater.* **2009**, *19*, 3165.
[5] H. B. Zeng, W. P. Cai, P. S. Liu, X. X. Xu, H. J. Zhou, C. Klingshirn, H. Kalt, *ACS Nano* **2008**, *2*, 1661.
[6] G. Z. Shen, Y. Bando, B. Liu, D. Golberg, C. Lee, *Adv. Funct. Mater.* **2006**, *16*, 410.
[7] C. Klingshirn, *Phys. Status Solidi B* **2007**, *244*, 3027.
[8] H. J. Zhou, J. Fallert, J. Sartor, R. J. B. Dietz, C. Klingshirn, H. Kalt, D. Weissenberger, D. Gerthsen, H. B. Zeng, W. P. Cai, *Appl. Phys. Lett.* **2008**, *92*, 132112.
[9] T. Makino, Y. Segawa, M. Kawasaki, A. Ohtomo, R. Shiroki, K. Tamura, T. Yasuda, H. Koinuma, *Appl. Phys. Lett.* **2001**, *78*, 1237.
[10] W. I. Park, G. C. Yi, M. Y. Kim, S. J. Pennycook, *Adv. Mater.* **2003**, *15*, 526.
[11] D. C. Look, B. Claflin, Y. I. Alivov, S. J. Park, *Phys. Status Solidi A* **2004**, *201*, 2203.
[12] W. I. Park, G. C. Yi, *Adv. Mater.* **2004**, *16*, 87.
[13] M. C. Jeong, B. Y. Oh, M. H. Ham, S. W. Lee, J. M. Myoung, *Small* **2007**, *3*, 568.
[14] R. Konenkamp, R. C. Word, M. Dosmailov, J. Meiss, A. Nadarajah, *Appl. Phys. Lett.* **2007**, *102*, 056103.
[15] H. Sun, Q. F. Zhang, J. L. Wu, *Nanotechnology* **2006**, *17*, 2271.
[16] W. Q. Yang, H. B. Huo, L. Dai, R. M. Ma, S. F. Liu, G. Z. Ran, B. Shen, C. L. Lin, G. G. Qin, *Nanotechnology* **2006**, *17*, 4868.

[17] Y. G. Cui, G. T. Du, Y. T. Zhang, H. C. Zhu, B. L. Zhang, *J. Cryst. Growth* **2005**, *282*, 389.
[18] T. Matsumoto, K. Nishimura, Y. Nabetani, T. Kato, *Phys. Status Solidi B* **2004**, *241*, 591.
[19] M. S. Oh, S. H. Kim, T. Y. Seong, *Appl. Phys. Lett.* **2005**, *87*, 122103.
[20] B. Q. Cao, W. P. Cai, H. B. Zeng, G. T. Duan, *J. Appl. Phys.* **2006**, *99*, 073516.
[21] X. D. Wang, J. H. Song, P. Li, J. H. Ryou, R. D. Dupuis, C. J. Summers, Z. L. Wang, *J. Am. Chem. Soc.* **2005**, *127*, 7920.
[22] M. Izaki, T. Omi, *Appl. Phys. Lett.* **1996**, *68*, 2439.
[23] S. Peulon, D. Lincot, *Adv. Mater.* **1996**, *8*, 166.
[24] T. Pauporte, D. Lincot, *Appl. Phys. Lett.* **1999**, *75*, 2861.
[25] T. Matsumoto, K. Nishimura, A. Nishii, A. Ota, Y. Nabetani, T. Kato, *Phys. Status Solidi C* **2006**, *3*, 984.
[26] H. Kumano, A. A. Ashrafi, A. Ueta, A. Avramescu, I. Suemune, *J. Cryst. Growth* **2000**, *214/215*, 280.
[27] H. B. Zeng, G. T. Duan, Y. Li, S. K. Yang, X. X. Xu, W. P. Cai, *Adv. Funct. Mater.* **2010**, *20*, 561.
[28] H. Zeng, W. Cai, Y. Li, J. Hu, P. Liu, *J. Phys. Chem. B* **2005**, *109*, 1826.

Received: May 12, 2010
Published Online: August 18, 2010

